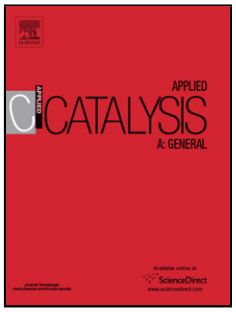

Title: Hexagonal zirconium phosphate nanoparticles as an
efficient and recyclable catalyst for selective solvent-free
alkylation of phenol with cyclohexanol

Author: Abdol Reza Hajipour Hirbod Karimi

PII: S0926-860X(14)00370-6
DOI: http://dx.doi.org/doi:10.1016/j.apcata.2014.05.036
Reference: APCATA 14856

To appear in: *Applied Catalysis A: General*

Received date: 18-1-2014
Revised date: 24-5-2014
Accepted date: 27-5-2014

Please cite this article as: A.R. Hajipour, H. Karimi, Hexagonal zirconium phosphate nanoparticles as an efficient and recyclable catalyst for selective solvent-free alkylation of phenol with cyclohexanol, *Applied Catalysis A, General* (2014), http://dx.doi.org/10.1016/j.apcata.2014.05.036

Hexagonal zirconium phosphate nanoparticles as an efficient and recyclable catalyst for selective solvent-free alkylation of phenol with cyclohexanol

Abdol Reza Hajipour [a,b,*] , Hirbod Karimi [a]

*Correspondence to: Abdol Reza Hajipour, Pharmaceutical Research Laboratory, Department of Chemistry, Isfahan University of Technology, Isfahan 84156, IR Iran. E-mail: haji@cc.iut.ac.ir

[a] Pharmaceutical Research Laboratory, Department of Chemistry, Isfahan University of Technology, Isfahan 84156, IR Iran

[b] Department of Neuroscience, University of Wisconsin, Medical School, Madison, WI 53706-1532, USA

Abstract

A facile synthesis of hexagonal α-zirconium phosphate (ZP) nanoparticles as an effective, eco-friendly and recyclable solid acid catalyst was studied. Polyvinylpyrrolidone (PVP) and Polyvinyl alcohol (PVA) were used as the organic matrix which were the dispersing agents and acted as a template for the nanoparticles. It seems H-bonds between ZP and PVA or PVP along polymer chains lead to a better dispersion of in situ formed ZP. Pure ZP nanoparticles with hexagonal shape were obtained after calcination of PVA/ZP or PVP/ZP. The catalysts were characterized by several physico-chemical techniques such as BET, ICP-OES, XRD, FT-IR, SEM and TEM. The TPD-NH_3 analysis suggests the presence of a reasonable amount of Brønsted acid sites. The acidic properties were studied in the alkylation of phenol with cyclohexanol under solvent-free conditions which produced 2-

cyclohexylphenol (2-CP), 4-cyclohexylphenol (4-CP) and 2,4-dicyclohexylphenol (2,4-DCP). This alkylation reaction was also performed over P_2O_5/Al_2O_3, P_2O_5/SiO_2, α-ZrP (prepared in the absence of the polymers) and various ionic liquids using cyclohexanol and cyclohexene as the alkylating agents. When the hexagonal ZP nanoparticles were used as the catalyst, under optimized reaction conditions, excellent conversion of phenol and selectivity toward 4-CP were obtained. The catalyst was recovered easily from the reaction mixture, regenerated and reused at least four times without significant loss in its catalytic activity.

Keywords: Hexagonal zirconium phosphate, Nanoparticles, Solvent-free, Solid acid catalyst, Cyclohexylphenol.

1. Introduction

Alkylation of phenols is one of the most important aromatic reactions, both in organic synthesis and chemical manufacturing. The alkylphenols are widely used as precursors in detergents, pesticides, additives for fuels, herbicides, polymers, phenolic resins, antioxidants, lubricants, fragrances, thermoplastic elastomers and paints [1-4]. Cyclohexylphenol is one of the very interesting alkylated phenol compounds. Cyclohexylation of phenol produces 2-cyclohexylphenol (2-CP), 4-cyclohexylphenol (4-CP), 2,4-dicyclohexylphenol (2,4-DCP), 2,6-dicyclohexylphenol (2,6-DCP) and cyclohexylphenyl ether (CPE), depending on both the catalyst and the reaction conditions. Based on previous researches, it is well known that C-alkylation requires stronger acid sites than those for O-alkylation [2-6]. In the cyclohexylation of phenol, the crucial point is the regioselectivity. 4-CP is widely used as an intermediate in the manufacture of colorants for plastics, biocides, dyes and 2-CP is an important intermediate in dyestuff and 2-phenylphenol preparation as a disinfectant [3-6]. This reaction has been performed over various catalysts such as zeolites [7,8], cationic ion-exchange resins [6], 12-tungstophosphoric acid [9], cesium salt of dodecatunstophosphoric acid [4], HZSM5 [10], $La_2(HPO_4)_3$, $BaSO_4$ and $SrSO_4$ [11], Silica-supported BF_3 [12], and acidic ionic liquids [13]. Traditionally, concentrated H_2SO_4 and H_3PO_4 [14,15] were used for cyclohexylation of phenol, but these homogeneous catalysts are not desirable as they are hazardous, corrosive and highly-polluting, and thus their usage leads to serious environmental problems. Moreover, in almost all these methods, lack of positional selectivity toward 4-CP, as the most desirable product have been reported. Hence, there is much interest for the development of more efficient and eco-friendly methods.

As a heterogeneous green solid acid catalyst, α-zirconium phosphate (ZP), $Zr(HPO_4)_2.H_2O$, is one of the most important inorganic materials which has been prepared by various methods [16,17]. Crystalline ZP is an important class of layered multi-functional materials with well-ordered structure. The layered structure of ZP consists of zirconium ions in a semiplanar arrangement, located slightly above and below the mean plane, while each Zr^{4+} ion is connected through the oxygen atoms of phosphate groups from above and below. Three of the four oxygen atoms in the phosphate groups are bonded to three different zirconium atoms. The fourth oxygen atom of the phosphate groups that bonds to a proton, the free –OH group, is pointing into the interlayer region (Scheme 1) [16-18]. These hydroxyl groups are responsible for ZP Brønsted acidity. The P-OH groups on the surface of ZP could be assumed as hooks in which various organic functional groups could adsorb on (acidic, polar, and hydrophobic), allowing to control both the reactivity and selectivity of the reaction.

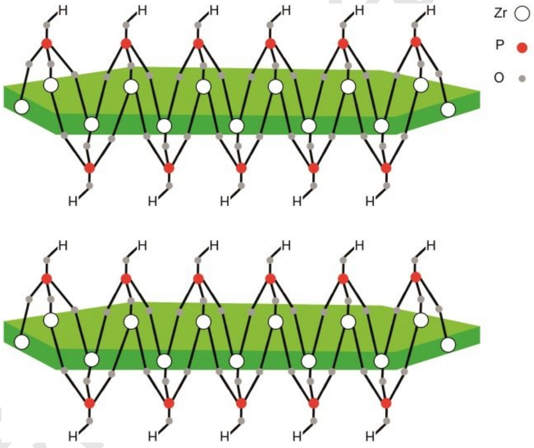

Scheme 1. Schematic structure of hexagonal α-zirconium phosphate.

Previous researches have shown potential applications of ZP in many fields [19-31]. ZP has attracted enormous interests as a low cost, efficient, thermally stable, acidic, eco-friendly and reusable catalyst [23-27]. It is an important ion exchanger [19,20] with high water tolerance ability and easy sedimentation [22] which also was used in nuclear waste management [20,21], drug delivery and immobilization of biological materials [28-31]. Recently, much attention has been focused on the development of new preparation methods to produce different ZP nano compounds such as nanoparticles [24,25,32,33], nanoplates

[17,30] and nanocomposites [34-36]. Polyvinylpyrrolidone (PVP) and Polyvinyl alcohol (PVA) are both white, water-soluble, odorless and nontoxic polymers. There are some new PVA and PVP based precursor methods to produce nanaocomposites and nanoparticles [33-40]. To the best of our knowledge, there is no report available in the literature for using ZP nanoparticles as catalyst for cycloalkylation of phenol and not much work has been reported on the alkylation of phenol using cyclohexanol. Therefore, in continuation of our researches to find efficient and green catalysts [41-44], we have investigated cycloalkylation of phenol by cyclohexanol over ZP nanoparticles under solvent-free conditions. The reaction conditions such as the amount of catalyst, reaction time, temperature and mole ratio were investigated in detail. Also, we have investigated this alkylation over a series of ionic liquids, P_2O_5/Al_2O_3, P_2O_5/SiO_2 and α-ZrP (prepared in the absence of the polymers). This alkylation reaction was performed with both cyclohexanol and cyclohexene as the alkylating agents and results were compared with those obtained from ZPA and ZPP.

2. Experimental

2.1 Catalyst synthesis

All Chemicals and solvents were purchased from Merck Chemical Company and used without further purification. The detailed procedure for the preparation of the catalyst can be found in the literature [33]. Typically, a 10% solution of PVA (Mw = 70000) was prepared by dissolving PVA in deionized hot water (95 °C). By adding HCl, the pH value was adjusted about 3. 50 ml of a 1 M solution of $ZrOCl_2.8H_2O$ added dropwise to precursor solution and heated at the 60 °C for 2 h with constant stirring using a magnetic stirrer. To the resulting homogeneous solution, under ultrasonication, 50 ml of a 2 M H_3PO_4 solution was added dropwise at 50-60 °C for 2 h. The resulted mixture was allowed to age for 4 h then the precipitate was filtered, washed several times with distilled water and then dried in an oven at 80 °C overnight. The obtained white colored fluffy precursor was ground and calcined at 550

°C for 4 h to decompose the organic matrix. The final product, the desired pure hexagonal α-zirconium phosphate ($Zr(HPO_4)_2.H_2O$) nanocrystals, was identified as ZPA.

A 10% solution of PVP (Mw = 40000) was prepared by dissolving of PVP in deionized water. The same procedure described above was performed to produce ZP nanoparticles. The final product was identified as ZPP. The detailed procedure for the preparation of the α-ZrP can be found in the literature [17]. P_2O_5/Al_2O_3 [45], P_2O_5/SiO_2 [46], 1-H-3-methyl-imidazolium bisulfate ([Hmim]HSO_4) [47], morpholinium bisulfate ([morH]HSO_4) [48], N-(4-sulfonic acid) butyl triethyl ammonium hydrogen sulfate ([TEBSA]HSO_4) [49] and 3-carboxypyridinium hydrogen sulfate ([Hcpy]HSO_4) [50] were prepared according to previously reported procedures by our research team (supplementary information). The gas chromatography-mass spectroscopy (GC-MS) analyses were performed by the Agilent 5975C spectrometer.

2.2. Catalyst characterization

On the basis of N_2 adsorption-desorption isotherms at liquid nitrogen temperature, the specific surface area was determined by BET [51] with a Quantachrome ChemBET 3000 (Fig. 1). Prior to analysis, each sample was degassed at 400 °C for 2 h to remove any adsorbed species on the surface. Total acidity of the samples was determined by temperature-programmed desorption of ammonia (TPD-NH_3) with a Quantachrome ChemBET 3000. Before the adsorption of ammonia, the samples were pre-treated in He at 250 °C for 30 min and then at 350 °C for 1 h and cooled to 100 °C. Then ammonia was adsorbed on the samples for 1 h. The TPD-NH_3 was carried out between 100 and 880 °C, at 10 °C min^{-1}, and analyzed by a thermal conductivity detector (TCD) for continuous monitoring of the desorbed ammonia. Typical curves of the release of NH_3 from ZP under different conditions are shown in Fig. 2. The Zr and P contents were obtained using inductivity coupled plasma-optical emission spectroscopy (ICP-OES) on PerkinElmer icp-oes 7300 dv spectrometer. The results are discussed in Section 3. The FT-IR spectroscopic measurements were carried out using a JASCO FT/IR (680 plus) spectrophotometer (Fig. 3). The spectra were recorded in the range 400–4000 cm^{-1} using a KBr technique. The crystallinity of ZPA and ZPP after calcination at 550 °C were measured by a Philips X'pert X-ray powder diffractometer. The samples were scanned in 2θ range of 5–50° (Fig. 4). The morphology of the samples was investigated using a Philips XL scanning electron microscope (SEM). Transmission electron microscope (TEM) images were collected using a LEO912-AB microscope.

2.3 Reaction procedure

The cyclohexylation of phenol was carried out in a 25 mL round bottom flask, equipped with a magnetic stirrer and water condenser. To minimize the evaporation, water was chilled to 2–3 °C by ice and circulated through the condenser by using a pomp. In a typical run, phenol (10 mmol) and ZP (pre-activated at 400 °C for 2 h and cooled in a desiccator to minimize moisture content) (50 mg, 0.17 mmol), were transferred into the reactor. To minimize the cyclohexanol vaporization and side reactions like dehydration of cyclohexanol to cyclohexene, when the reaction temperature reached 80 °C, cyclohexanol (10 mmol) was added. To optimize the reaction conditions, similar reactions were performed by varying phenol/cyclohexanol mole ratio, reaction time, the amount of catalyst and temperature. Samples were collected periodically and analyzed by GC. The reaction mixture was cooled at the end, diluted by *n*-hexane (5 ml) and then, the catalyst was recovered by centrifuge. The organic phase was dried over $MgSO_4$ and then analyzed by GC-MS. Alkylation of phenol resulted in a mixture of three different products: 2-CP, 4-CP and 2,4-DCP that have shown in Scheme 2. No CPE or 2,6-DCP was detected. Also, different alkylation reactions, as described above, were performed over P_2O_5/Al_2O_3 and P_2O_5/SiO_2 (pre-activated at 120 °C for 2 h) (10 mol%), [Hmim]HSO_4 (20 mol%), [morH]HSO_4 (10 mol%), [TEBSA]HSO_4 (5 mol%) and [Hcpy]HSO_4 (7 mol%). The results were compared with those obtained from ZPA and ZPP (supplementary information).

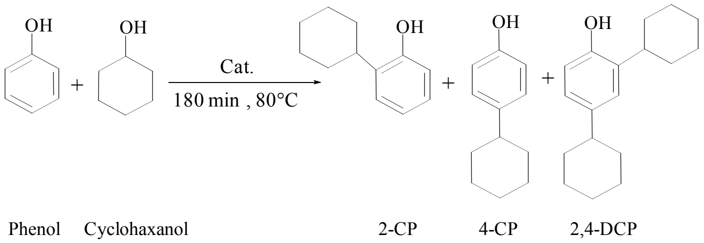

Scheme 2. The products of phenol alkylation with cyclohexanol under optimized reaction conditions.

The conversion of reactants and selectivity of the desired products were calculated on the basis of its mol percent using GC data as follows:

$$\% \text{ conversion} = \frac{[100 \times (\text{initial mol\%} - \text{final mol\%})]}{\text{initial mol\%}}$$

$$\% \text{ selectivity} = \frac{[\text{GC peak area \% of the desired product}]}{\sum \text{total GC peak area \% of all products}}$$

Gas chromatography analyses were performed under the conditions: 30 m Agilent J&W HP-5 chromatography column (30m, 0.32 mm, 0.25 µm GC Column), initial temperature 80 °C, ramp rate 20 °C/min, final temperature 300 °C, injector 300 °C, FID detector 320 °C and 1-heptanol was used as an internal standard.

2.4 Catalyst regeneration

In order to examine the recyclability of the catalyst, used ZPA (ZPP) was recovered from the reaction media and re-used. For recycling, after the first use, the catalyst was separated from the reaction mixture by centrifuge, washed with ethanol successively and refluxed with 15% (w/v) H_2O_2 for 2 h. It was then washed with water, dried at 120 °C for 2 h and finally activated at 450 °C for 2 h [23,25]. The regenerated catalyst was used under the optimum reaction conditions to study the performance of recovered catalyst. After every reaction cycle the catalyst was recovered, washed and activated as described above.

3. Results and discussion

On addition of phosphate ions into the PVA/Zr^{4+} or PVP/ Zr^{4+} solutions, the formation of ZP began immediately. PVA and PVP were used as the dispersing agent, organic matrix and also acted as a template for the nanoparticles. H-bond interactions between anchored polar groups of PVA and PVP with the P-OH groups of ZP play an important role in the better distribution of ZP. After calcinations of PVA/ZP or PVP/ZP at 550 °C for 4 h and decomposition of the organic matrix, pure ZP nanoparticles with hexagonal shape were obtained. Alkylation of aromatics over solid catalysts is known to occur either by the adsorption of both the aromatic and the alkylating agent molecules on the surface i.e., by a Langmuir–Hinshelwood (LH) mechanism or by the reaction of the adsorbed alkylating agent with aromatic molecules in the gas phase, i.e., by an Eley–Rideal (ER) mechanism [10,51-53]. From the product distribution the following mechanism can be proposed for the alkylation reaction. At first, it seems cyclohexanol and phenol are adsorbed on the ZPA (or ZPP) surface due to hydrogen bonding. In the presence of ZPA (or ZPP) as solid acid catalysts, cyclohexanol turns to cyclohexyl cation which is so reactive toward nucleophiles, such as phenol, which produces 2-CP, 4-CP and 2,4-DCP (Scheme 2). The main advantage of ZPA (or ZPP) as an alkylating catalyst, in comparison with other catalysts, is that it can significantly influence the product selectivity due to its uniform structure.

3.1. Characterization of catalysts

There were no significant differences between the analytical results of ZPA and ZPP. Table 1 represents the ICP data, in where the P/Zr ratio was found to be 1.82, 1.89 and 1.66 for ZPA, ZPP and α-ZP, respectively [24,25].

Table 1. Element contents of zirconium phosphates (at.%).

Samples	O	Zr	P
ZPA	70	10.6	19.4
ZPA[a]	68.7	11.6	19.7
ZPA[b]	61.9	14.8	23.3
ZPP	71	10.	19

ZPP[b]	61.3	14.9	23.8
α-ZP	73.4	10	16.6

[a] After the first cycle.
[b] After the 5th cycle.

The isotherm shows three adsorption stages. The first stage is in $P/P_o<0.35$, the second stage is in the range of $0.35<P/P_o<0.85$ near horizontal section, and a third stage in higher partial pressure ($P/P_o>0.85$). The isotherm resembles the type (IV) isotherms [54]. The surface area was found to be 118.2 and 117.1 m^2g^{-1} for ZPA and ZPP, respectively. The increase in adsorption at higher relative pressure (P/P_o) showed the presence of larger size mesoporous in the sample [27,55,56]. As it can be seen from Fig. 1a and 1b, both the N_2 adsorption–desorption isotherm curves are quite similar.

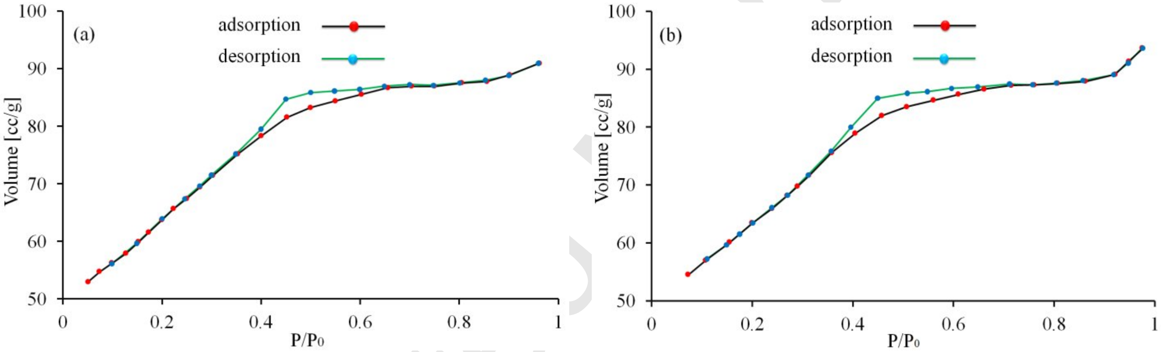

Fig. 1. Nitrogen adsorption–desorption isotherms for ZPA (a) and ZPP (b).

TPD-NH_3 provides a quantitative estimation of the total number of acid sites and the distribution of acid strengths. Because of the strong basicity of NH_3 gas, it was expected that all acid sites on the catalysts interact with NH_3. The total amount of NH_3 desorbed after saturation permits the quantification of the number of acid sites on the surface, while the position of the peak, desorption temperature, indicates the strength of the catalyst, i.e., the higher temperature of desorption, the stronger the acid strength. The TPD-NH_3 curves of fresh (blue lines) and used (red dashes) ZPA and ZPP are shown in Fig. 2a and 2b. The characteristic TPD curves of both samples are quite similar. Judging from the temperatures at which the maximum amount of NH_3 desorbed from the samples, ZPA and ZPP both have strong acidity. ZPA and ZPP desorbed ammonia in a wide range of temperatures from 170 to

880 °C, which mostly corresponds to the medium and the strong acidic sites. The NH_3 desorption peak at temperatures below 250 °C belongs to the physisorption/chemisorptions of NH_3 molecules on weak acidic sites. The peak at about 250-450 °C shows the existence of intermediate strength acidic sites and finally the peak at 450-880 °C demonstrates the presence of strong acidic sites on the surface of ZPA and ZPP [57,58]. The NH_3-TPD curves of ZPA (Fig. 2a) and ZPP (Fig. 2b) exhibit the presence of significant amounts of strong acid sites. Fig. 2a and 2b (blue lines) show that the desorption of ammonia starts at almost 190 and 178 °C, centered at 423 and 430 °C with a small hump at about 333 and 341 °C for ZPA and ZPP, respectively. The NH_3-TPD curves subsequently decreased with further increase in temperature and did not complete even at 880 °C for both ZPA and ZPP. This indicates that ZPA and ZPP contain a considerable number of strong acid sites which are attributed to the presence of P-OH groups on the surface of zirconium phosphate layers and make them suitable solid acid catalysts [23-27]. The extent of desorptions is found to be ca. 2.1 and 1.93 mmol NH_3/g of catalyst for ZPA and ZPP, respectively.

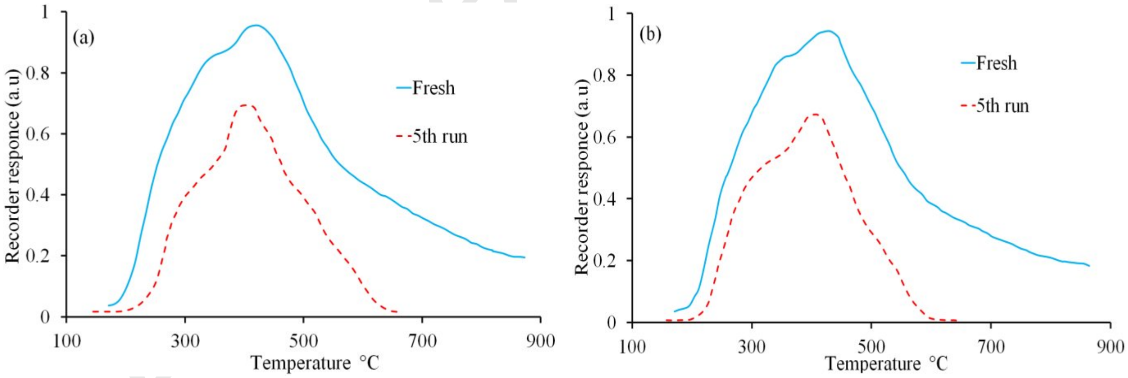

Fig. 2. NH_3 TPD profile of ZPA (a) and ZPP (b), fresh (blue line) and after the 5th run (red dashes).

A TPD experiment was carried out after the 5th cycle by recovering the catalysts, in order to magnify the difference from the fresh catalysts. Fig. 2a and 2b (red dashes) reveals the TPD-NH_3 curves of ZPA and ZPP after the 5th run. The comparison of the TPD curves before and after catalysis on the same sample of ZPA and ZPP shows a decrease of strong acid sites and an increase of medium/weak acid sites after the 5th run. Furthermore, the total concentration of acid sites of the used ZPA and ZPP (Table S1 supplementary information) decreased with the decrease of surface area (section 3.2.5). The obtained results were compared with previous reports [18,25,56]. The FT-IR spectra of the calcined ZPA and ZPP are shown in Fig. 3. They were in agreement with earlier reports [33,56-59]. The main characteristic bands are 3366 (3360), 1626 (1621), 1062 (1042) and 597 (594) cm^{-1}. The strong broad-sharp band with peak maxima appearing at 1062 (1042) cm^{-1} corresponded to the P–O symmetrical stretching vibration of PO_4^{3-}. The broad peak with peak maxima at 3366 (3360) and the sharp peak at 1626 (1621) cm^{-1} in the spectrum of calcined ZPs are attributed to surface asymmetric OH stretching and bending of the water molecule, respectively. The broad band around 3400 cm^{-1} is actually an envelope of peaks due to PO–H stretching of many P-OH types [56]. The spectra showed bands located at 597 (594) cm^{-1} which were assigned to Zr–O bonds.

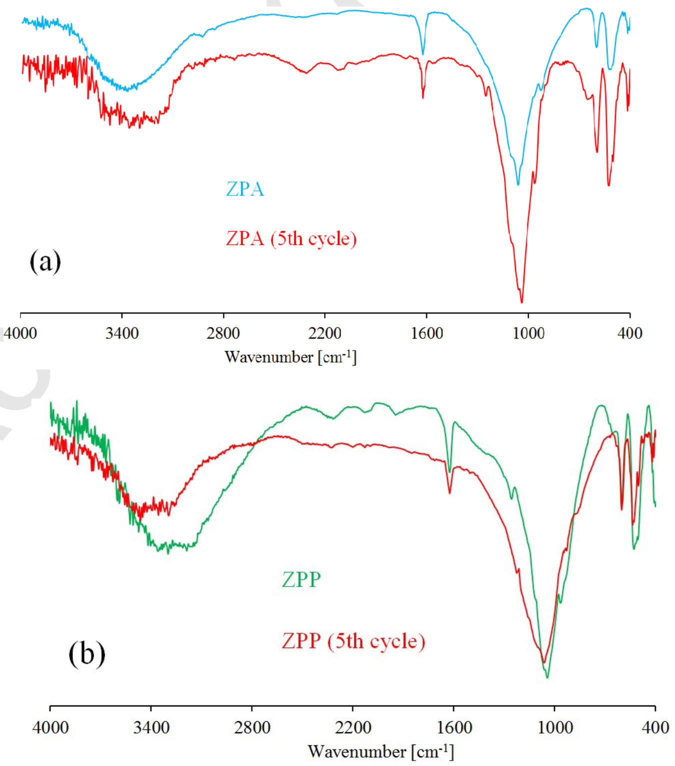

Fig. 3. FT-IR spectra of ZPA (a) and ZPP (b) before and after use.

Fig. 4 shows the powder XRD patterns of the prepared ZPA and ZPP. It shows some characteristic reflections in the 2θ range of 5–50° that represents the structure of the ZP. The peak at 2θ ~ 12° indicates a spacing of 7.4 A° for the planes and the reported refined crystal structure of ZP [16,17,33,57-59]. Therefore, from the above data, formation of ZP was concluded.

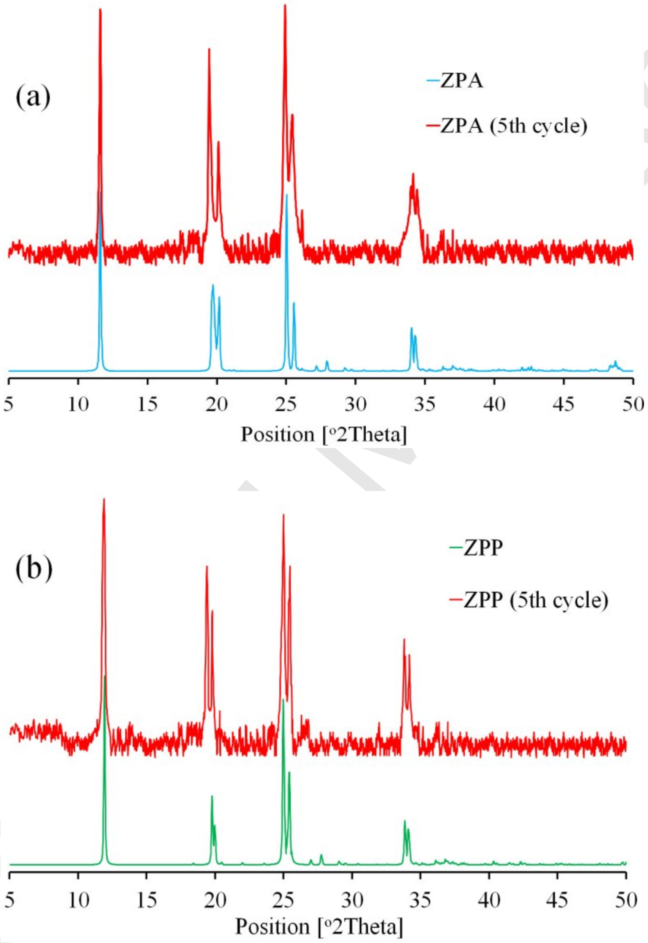

Fig. 4. XRD patterns of powder ZPA (a) and ZPP (b) before and after use.

The morphology of the ZP nanoparticles was characterized by SEM [33,56-59] and TEM [25,32,33,56]. Typically, the SEM micrograph of ZPs shows the hexagonal plates in which the disks had well-defined shapes with very smooth surface. The morphology of both solids is almost identical and solid layers are placed parallel, showing good crystallinity. However, there are some incomplete plates which are ellipse. The TEM images show that the particles are hexagonal with smooth surfaces. Because of the condensation reactions between hydroxyl groups of adjacent particles during aging or calculation, particles in some cases are attached together which cause more agglomeration. The average diameter of ZP nanoparticles is about 60 nm. SEM and TEM results of all the calcined ZPs samples show similar uniform morphology and are in fair congruence with the earlier reports [25,32,56-59]. For a detailed discussion, please refer to our previous report [33].

3.2. Cycloalkylation of phenol over ZPA (ZPP): influence of experimental parameters

Cyclohexylation of phenol using cyclohexanol (and cyclohexene) was performed over ZPA (ZPP) nanoparticles by varying the reaction parameters such as the amount of catalyst, reaction time, temperature and reactants mole ratio. The obtained products were 2-CP, 4-CP and 2,4-DCP. Scheme 2 shows the reaction and the detected products under optimized reaction conditions. No 2,6-DCP and CPE were detected. Since both ZPA and ZPP are α-zirconium phosphate ($Zr(HPO_4)_2.H_2O$) nanocrystals, there is no difference between their analytical results or catalytic activities.

3.2.1 The effect of catalyst mass

The reaction was carried out with different amount of catalyst within the range of 10–60 mg under the following conditions: temperature 80 °C, reaction time 180 min and phenol/cyclohexanol mole ratio 1:1. The % conversion of phenol, cyclohexanol and % selectivity of different products are summarized in Fig. 5. It is evident from Fig. 5 that with an increase in the amount of catalyst, the % conversion of phenol was also increased. When the ZAP (ZPP) mass was increased from 10 to 50 mg the conversion of phenol increased from 52 (53) to 93 (92) %, which is obviously due to the proportional increase in the number of active sites. More available acid sites cause formation of more cyclohexyl cations, which increased the conversion of the phenol. Also, the % conversion of cyclohexanol was increased from 65 (62) to 96 (96) %, when the ZPA (ZPP) mass was increased. Acid catalyzed alkylation by alcohol or alkene is known to occur by the nucleophilic attack of the aromatic substrate on carbocation intermediate [5,8]. The carbocation intermediate is generated by the protonation and subsequent dehydration of alcohol or direct protonation of the alkene [60]. The strong Brønsted acid sites in ZPA (ZPP) could protonate the hydroxyl group in cyclohexanol to form the oxonium ion which can easily liberate H_2O molecule to form the cyclohexyl carbocation [5,7,8,]. The formed carbocation could either directly attack the ortho or para position of phenol to give the ortho or para alkyl phenol. The carbocation can produce cyclohexene by elimination of a proton, which can also be an alkylating agent under the reaction condition [7,8].

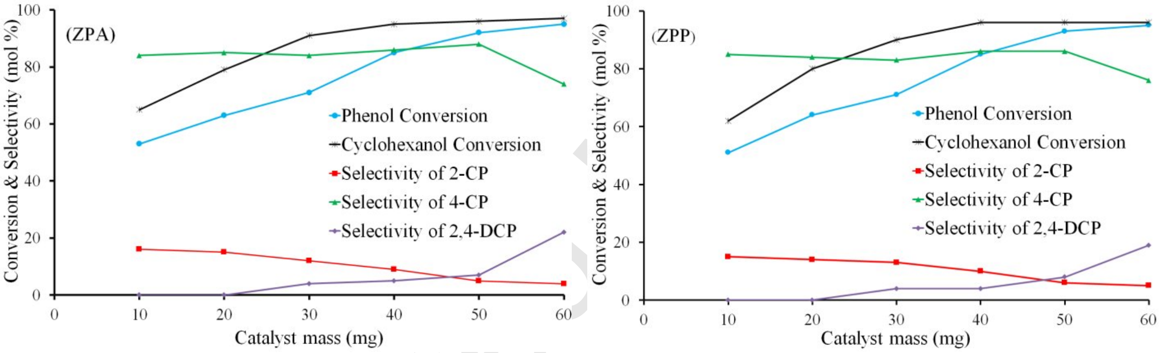

Fig. 5. Variation of reactants conversion and selectivity to main reaction products with ZPA and ZPP mass amount. The reaction conditions: phenol/cyclohexanol = 1:1, 180 min and 80 °C.

Since ZPA (ZPP) surface is full of hydroxyl groups (P-OH), it is very possible for both phenol and cyclohexanol to have effective interactions with those hydroxyl groups (probably due to H bonding) [61,62]. This may lead to specific orientation and explains such product distribution. When the phenol is adsorbed on the surface of ZPA (ZPP), there is more steric hindrance around the ortho position (near the catalyst surface), but less steric hindrance around the para position. As a result, there is low selectivity toward 2-CP. Besides, no 2,6-DCP was detected. Product distribution also varied with the amount of catalyst. As the catalyst amount was increased, due to availability of more acid sites, both 2-CP and 4-CP could undergo for the secondary alkylation to produce 2,4-DCP. Further amount of ZPA or

ZPP (60 mg) increased % conversion of phenol slightly, but decreased % selectivity of 4-CP sharply (Fig. 5). Hence, 50 mg of ZPA (ZPP) was chosen as the appropriate catalyst mass for further experiments. As evidenced in Fig. 5, there is no significant difference between ZPA and ZPP results in this alkylation reaction.

3.2.2. The effect of time

Fig. 6 shows the effect of reaction time on the % conversion and % selectivity of cycloalkylation of phenol at 80 °C, 50 mg of ZPA (ZPP) and the phenol/cyclohexanol mole ratio of 1:1. As can be seen from this figure, an increase in the reaction time (30 to 210 min), cause an increase in conversion of phenol and cyclohexanol. When ZPA was used as catalyst, the conversion of phenol and cyclohexanol increased from 18 to 93% and 32 to 96% during reaction times of 30 to 180 min, respectively. Similarly, when the ZPP was used as catalyst, almost the same increase in the conversion of phenol (from 20 to 92%) and cyclohexanol (33 to 96%) was observed. Due to the consumption of cyclohexanol in the reaction media, fewer molecules are left in the reaction mixture and more time is required to generate the cyclohexyl cations from the cyclohexanol.

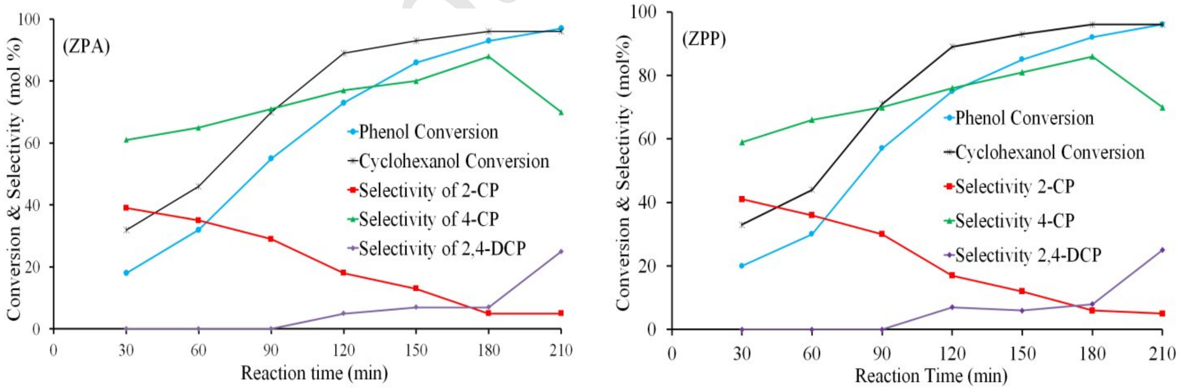

Fig. 6. Variation of reactants conversion and selectivity to main reaction products with time. The reaction conditions: phenol/cyclohexanol/catalyst = 1:1:0.017 and 80 °C.

Further, initial rate of desorption of the products from the catalyst surface is high and as the concentration of the products increases in the reaction mixture the rate becomes slow.

Also, there is a decrease in the selectivity of 2-CP during the first 180 min of reaction and increase in 4-CP, as the main product. Consequently, there is a decrease in the formation of 4-CP and an increase in the formation of 2,4-DCP. This may be because of isomerization of 2-CP to 4-CP and more available time for the initial products, 2-CP or 4-CP, to form 2,4-DCP by one additional cycloalkylation step [1,7,8,63]. Thus, prolonging the reaction time was not beneficial for the synthesis of 4-CP, however, conversion of phenol increased further. Therefore, 180 min was chosen as appropriate reaction time for further studies under current reaction conditions (Fig. 6).

3.2.3 The effect of reaction temperature

The alkylation of phenol with cyclohexanol was carried out in the temperature range 40 – 100 °C over ZPA (ZPP) (Fig. 7). Temperature has a prominent effect on the % conversion of phenol and cyclohexanol as well as distribution of the products. As temperature increased from 40 to 80 °C, the conversion of phenol sharply increased from 36 to 93% and 37 to 92% for ZPA and ZPP, respectively. Also, when the temperature increased, the % conversion of cyclohexanol was increased from 52 to 98% and 53 to 98% for ZPA and ZPP, respectively. The higher conversion of cyclohexanol at higher temperatures may be due to its dehydration to cyclohexene, which can also convert to cycloalkeyphenols [7,8]. At higher temperatures (90 and 100 °C), a small decrease of phenol conversion was observed (86% for ZPA and 85% for ZPP), which may be due to dealkylation or side reactions like poly-alkylation of cyclohexylphenols to 2,4-DCP [1,5,7,13]. It can be seen from Fig. 7, that the results for both catalysts are quite the same. When ZPA was used as the catalyst, the selectivity of 2-CP decreased (varies from 43% at 40 °C to 5% at 80 °C) and that of 4-CP increased (varies from 57% at 40 °C to 88% 80 °C) with temperature. This could be due to isomerization [7,8,13,64]. However, the selectivity towards 4-CP decreased from 88% at 80

°C to 61% at 100 °C with a parallel increase in the selectivity of 2,4-DCP, confirming the further alkylation reactions at higher temperature [7,8,13,64].

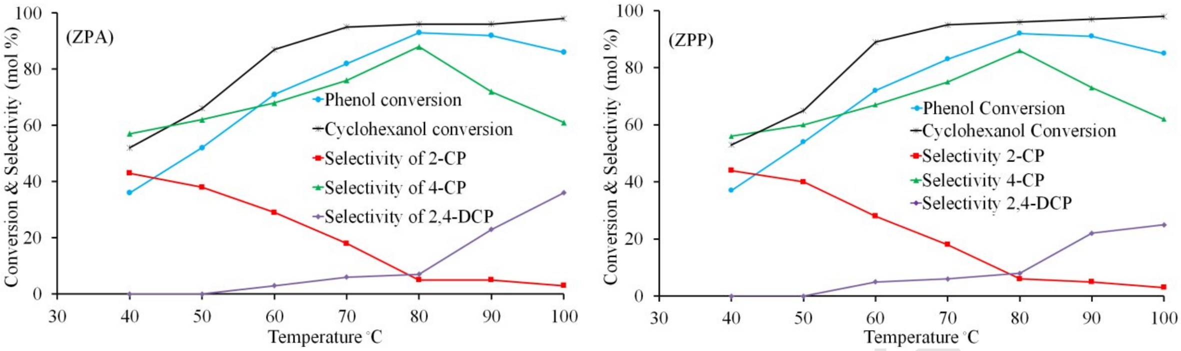

Fig. 7. Variation of phenol conversion and selectivity to main reaction products with reaction temperature. The reaction conditions: phenol/cyclohexanol/catalyst = 1:1:0.017 and 180 min.

The same changes in the selectivity of 2-CP, 4-CP and 2,4-DCP were observed for ZPP (Fig. 7). Therefore, the optimum reaction temperature was determined at 80 °C with respect to phenol conversion and product selectivity.

3.2.4 The effect of concentration of reactants

A series of experiments were carried out to establish the effect of reactant ratio on conversion and selectivity by varying the mole ratio of the phenol/cyclohexanol mole ratio from 3:1 to 1:4, by keeping all other conditions constant (Fig. 8). It can be seen that cyclohexanol conversion increased progressively when the mole ratio of phenol/ cyclohexanol was varied from 1:4 to 1:1. For both catalysts, 96% conversion of cyclohexanol was obtained, when the mole ratio of phenol/cyclohexanol was 1:1. When the mole ratio of cyclohexanol/phenol increased, the % conversion of phenol and the % selectivity towards 4-CP decreased, whereas the % selectivity towards 2,4-DCP increased. The catalyst active sites may be blocked due to higher cyclohexanol concentration as well as water adsorption. This was obtained from the cyclohexyl cation production, and as a result, conversion of phenol decreased. Lower selectivity toward 4-CP may be due to the higher concentration of the cyclohexanol as the alkylating agent in the reaction medium. Because of higher concentration of cyclohexanol, more cyclohexyl cations are available for reaction with 2-CP and 4-CP, which results in more 2,4-DCP product. Nevertheless, when the mole ratio varied to 3:1, the cyclohexanol conversion decreased (88 and 86% for ZPA and ZPP, respectively).

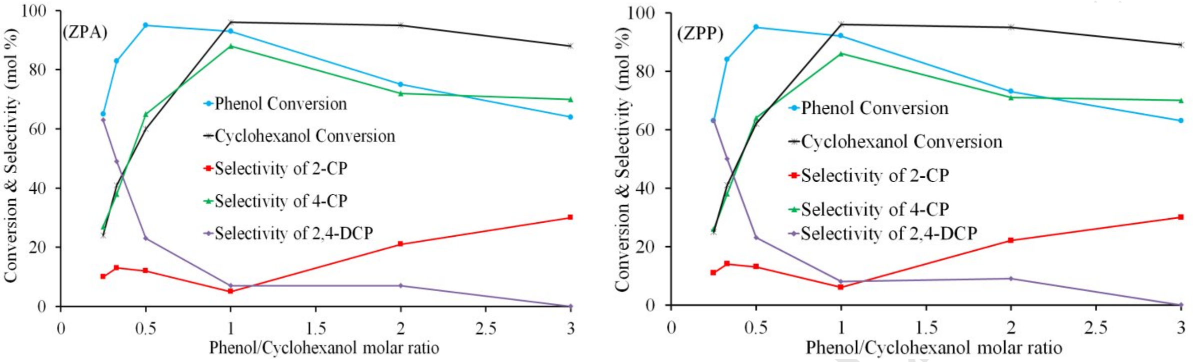

Fig. 8. Variation of reactants conversion and selectivity to main reaction products with reactants mole ratio. The reaction conditions: 180 min, 80 °C and 50 mg of catalyst.

Also, as seen in this figure, with an increase in the amount of the phenol, there is a decrease in the % conversion of phenol and % selectivity toward 4-CP. As the number of each reactant molecule increases on the surface of the catalyst (ZPA or ZPP), less sites remain available for the other reactant. No 2,4-DCP was detected when the mole ratio of phenol/cyclohexanol was 3:1. Thus, the optimum mole ratio was found to be 1:1 (Fig. 8).

3.2.5. Recyclability studies of catalyst

The regenerated ZPA and ZPP were characterized for their chemical composition by elemental analysis. No significant change in the composition or environment of the phosphate groups in ZPA (ZPP) was observed after regeneration (Table 1) (*only till the 5th cycle*). The catalysts were used again under the optimum reaction conditions and the results are summarized in Fig. 11 (also see Fig. S4). The recycled catalysts showed almost the same behavior as the fresh ones, but only up to 5th cycle. After that, the conversion of phenol decreased sharply from 93 to 73% and 92 to 71% for ZPA and ZPP, respectively (Fig. 9). The conversion of cyclohexanol also decreased after the 5th cycle. The lowered activity of reused catalyst confirms catalyst deactivation during the reaction.

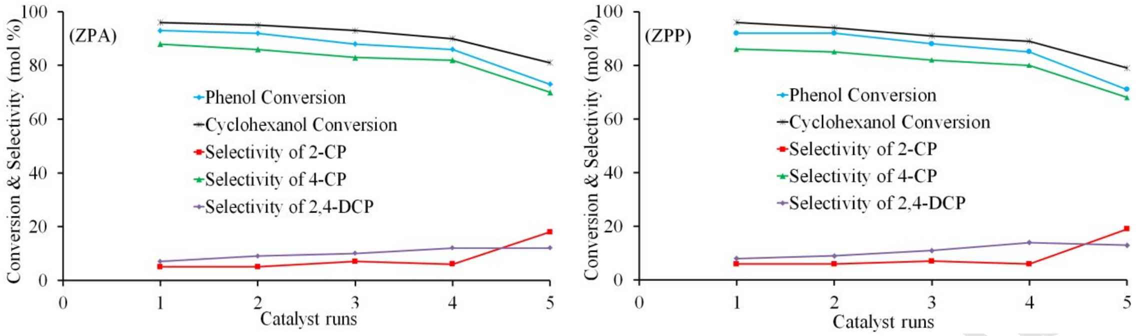

Fig. 9. Variation of reactants conversion and selectivity to main reaction products with reusability of ZPA and ZPP. The reaction conditions: phenol/cyclohexanol/catalyst = 1:1:0.017, 180 min and 80 °C.

It could be seen from Fig. 9 that the ZPA (ZPP) was utilized repeatedly over four times without any apparent loss of conversion and selectivity. Although, refluxing and thermal activation of regenerated catalysts cuased more agglomeration, which decreased the catalytic activitiy of the catalysts. Fig. 10a and 12b show the SEM and TEM images of ZPA after the 5th run, respectively. As mentioned before, agglomeration may be due to the condensation reactions between hydroxyl groups of adjacent particles. It seems that agglomeration of plates increased the average diameter particles (about 85-110 nm). ZPA (ZPP) surface area was also reduced to 70.1 (69.2) m^2g^{-1}. Moreover, condensation between hydroxyl groups decreases the number of acid sites on the catalyst. The extent of desorptions are found to be ca. 1.0 and 0.96 mmol NH_3/g of catalyst for ZPA and ZPP, respectively.

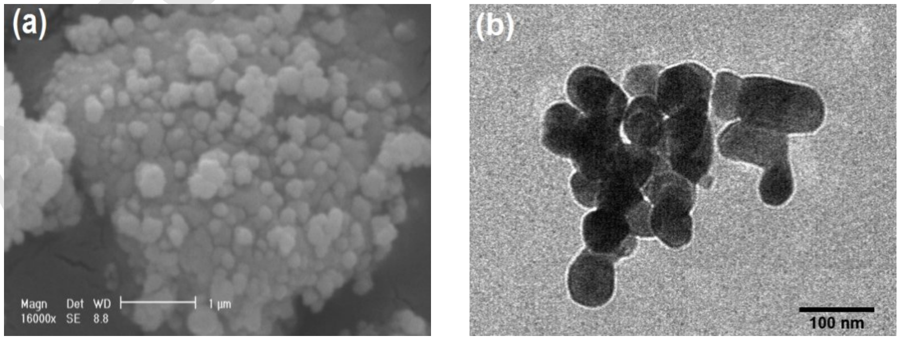

Fig. 10. SEM (a) and TEM (b) images of ZPA after the 5th run.

3.3 Comparison of activities of various catalysts

Table 3 shows a comparison between the catalytic activity of some catalysts which were used for this alkylation reaction in previous literatures. Of course, the reaction conditions are different, but the catalysts used in this study (ZPA and ZPP) might be one of the best catalysts with regards to lower reaction time and temperature, better phenol conversion and selectivity toward 4-CP. The catalysts can also be easily regenerated for further applications.

Table 3. Comparison between ZPA, ZPP and the other catalysts for phenol conversion and 4-CP selectivity.

Catalyst	Conversion (mol %)[a]	Time (min)	T (°C)	Product selectivity (%)					Ref.
				CPE	2-CP	4-CP	PCPs [b]	others	
ZPA	93	180	80	-	5	88	7	-	This work
ZPP	92	180	80	-	6	86	8	-	This work
TSA/ZrO_2	100 [c]	360	80	-	61	39	-	-	[1]
TSA/Al_2O_3	100 [c]	360	80	-	66	34	-	-	[1]
Sulfated zirconia	31.59	240	60	66.4	20.56	2.86	-	10.18	[2]
(20%w/w) DTP-HMS	70	240	60	63.3	23.4	130	-	-	[2]
Hβ-120	93.4 [d]	180	160	-	53	47	-	-	[5]
U-550 zeolite	83.2	360	200	4.1	15.6	42.7	17.9	19.7	[7]
HY zeolite	85	360	200	3	15.9	38.7	21.9	20.5	[7]
γ-Al_2 O_3	51.5	360	200	1.6	4.2	0.8	-	93.3[e]	[8]
Silica − alumina	54.2	360	200	28.9	7.7	1.3	1	61.1[e]	[8]
TPA/ZrO_2	100 [c]	360	80	-	69	31	-	-	[9]
Acidic Ionic Liquid	75.5	360	200	-	14	61.6	10	14.4	[13]
H_3PO_4	98	150	145	1	46	38	15	-	[22]
KU-2-FPP	95	150	130	5	69	25	2	-	[22]
Starbon®-COOH	85	48 (h)	110	78	5	17	-	-	[61]

[a] Conversion of phenol.
[b] PCPs: Poly cyclophenols.
[c] Cyclohexene conversion.
[d] Cyclohexanol conversion.
[e] Cyclohexene as the major product.

4. Conclusions

Hexagonal zirconium phosphate nanoparticles were synthesized and characterized by various methods. We have demonstrated that ZPA (ZPP) is an efficient and recyclable catalyst for the cycloalkylation of phenol at low temperature. In almost all cases, 4-CP was formed as the major product along with small amounts of 2-CP and 2,4-DCP. The optimum reaction conditions for this alkylation reaction were 80 °C; 180 min; phenol/cyclohexanol 1:1 and 50 mg of ZPA (ZPP). It seems that the surface of ZPA (ZPP) with hooky hydroxyl groups (P-OH) plays an important role in the selectivity of the reaction by interacting with hydroxyl groups of cyclohexanol and phenol.

Acknowledgments

We gratefully acknowledge the funding support received for this project from the Isfahan University of Technology (IUT), IR Iran. Further financial support from the Center of Excellence in Sensor and Green Chemistry Research (IUT) is gratefully acknowledged**.** The authors are also thankful to Dr. G. Azizi and Dr. M. Moshref javadi for valuable discussions**.**

References

[1] N. Bhatt, A. Patel, J. Mol. Catal. A: Chem. 264 (2007) 214-219.

[2] G.D. Yadav, G.S. Pathre, J. Mol. Catal. A: Chem. 243 (2006) 77-84.

[3] V. Krishnan, K. Ojha, N.C. Pradhan, Org. Process Res. Dev. 6 (2002) 132-137.

[4] G.D. Yadav, P. Kumar, Appl. Catal. A. 286 (2005) 61-70.

[5] V.P. Raje, R.P. Bhat, S.D. Samant, J. Mol. Catal. A: Chem. 240 (2005) 172-177.

[6] A. Chakrabarti, M.M. Sharma, React. Polym. 17 (1992) 331-340.

[7] R. Anand, K. Gore, B. Rao, Catal. Lett. 81 (2002) 33-41.

[8] R. Anand, T. Daniel, R.J. Lahoti, K.V. Srinivasan, B.S. Rao, Catal. Lett. 81 (2002) 241-246.

[9] N. Bhatt, A. Patel, Indian J. Chem. Sect. A. 47 (2008) 387.

[10] S.R. Kirumakki, N. Nagaraju, K.V.R. Chary, S. Narayanan, J. Catal. 221 (2004) 549-559.

[11] R. Pierantozzi, A.F. Nordquist, Appl. Catal. 21 (1986) 263-271.

[12] K. Wilson, D.J. Adams, G. Rothenberg, J.H. Clark, J. Mol. Catal. A: Chem. 159 (2000) 309-314.

[13] H.B. Yu, J. Nan, J.C. Zhang, J.Z. Gui, Adv. Mater. Res. 233-235 (2011)188-193.

[14] M.V. Postnova, S.G. Koshel, N.V. Lebedeva, E.A. Kuznetsova, G.N. Koshel, Russ. J. Org. Chem. 39 (2003) 1415-1417.

[15] M. Seino, S. Okazaki, T. Saito, Bull. Jpn. Pet. Inst. 18 (1976) 32-38.

[16] L. Sun, W.J. Boo, H.-J. Sue, A. Clearfield, New J. Chem. 31 (2007) 39-43.

[17] L. Sun, W.J. Boo, R.L. Browning, H.-J. Sue, A. Clearfield, Chem. Mater. 17 (2005) 5606-5609.

[18] C. Trobajo, S.A. Khainakov, A. Espina, J.R. García, Chem. Mater. 12 (2000) 1787-1790.

[19] S. Ahrland, J. Albertsson, A. Oskarsson, A. Niklasson, J. Inorg. Nucl. Chem. 32 (1970) 2069-2078.

[20] S.P. Mishra, D. Tiwari, S.K. Prasad, R.S. Dubey, M. Mishra, J. Radioanal. Nucl. Chem. 268 (2006) 191-199.

[21] N.Y. Kremlyakova, V.M. Komarevsky, J. Radioanal. Nucl. Chem. 218 (1997) 197-200.

[22] Y. Kamiya, S. Sakata, Y. Yoshinaga, R. Ohnishi, T. Okuhara, Catal. Lett. 94 (2004) 45-47.

[23] A. Sinhamahapatra, N. Sutradhar, S. Pahari, H.C. Bajaj, A.B. Panda, Appl. Catal. A. 394 (2011) 93-100.

[24] A. Sinhamahapatra, N. Sutradhar, B. Roy, P. Pal, H.C. Bajaj, A.B. Panda, Appl. Catal. B. 103 (2011) 378-387.

[25] A. Sinhamahapatra, N. Sutradhar, B. Roy, A. Tarafdar, H.C. Bajaj, A.B. Panda, Appl. Catal. A. 385 (2010) 22-30.

[26] F. Zhang, Y. Xie, W. Lu, X. Wang, S. Xu, X. Lei, J. Colloid Interface Sci. 349 (2010) 571-577.

[27] A. Sinhamahapatra, A. Sinha, S.K. Pahari, N. Sutradhar, H.C. Bajaj, A.B. Panda, Catal. Sci. Technol. 2 (2012) 2375-2382.

[28] A. Díaz, A. David, R. Pérez, M.L. González, A. Báez, S.E. Wark, P. Zhang, A. Clearfield, J.L. Colón, Biomacromolecules. 11 (2010) 2465-2470.

[29] V. Saxena, A. Diaz, A. Clearfield, J.D. Batteas, M.D. Hussain, Nanoscale. 5 (2013) 2328-2336.

[30] A. Díaz, V. Saxena, J. González, A. David, B. Casañas, C. Carpenter, J.D. Batteas, J.L. Colón, A. Clearfield, M.D. Hussain, Chem. Commun. 48 (2012) 1754-1756.

[31] C.V. Kumar, A. Chaudhari, J. Am. Chem. Soc. 122 (2000) 830-837.

[32] Y. Feng, W. He, X. Zhang, X. Jia, H. Zhao, Mater. Lett. 61 (2007) 3258-3261.

[33] A.R. Hajipour, H. Karimi, Mater. Lett. 116 (2014) 356-358.

[34] V.K. Gupta, D. Pathania, P. Singh, B.S. Rathore, P. Chauhan, Carbohydr. Polym. 95 (2013) 434-440.

[35] S. Wei, M. Lizu, X. Zhang, J. Sampathi, L. Sun, M.F. Milner, High Perform. Polym. 25 (2013) 25-32.

[36] Y. Yang, C. Liu, P.R. Chang, Y. Chen, D.P. Anderson, M. Stumborg, J. Appl. Polym. Sci. 115 (2010) 1089-1097.

[37] H. Lu, C.A. Wilkie, M. Ding, L. Song, Polym. Degrad. Stab. 96 (2011) 1219-1224.

[38] M. Aleahmad, H.G. Taleghani, H. Eisazadeh, Synth. Met. 161 (2011) 990-995.

[39] R. Topkaya, U. Kurtan, A. Baykal, M.S. Toprak, Ceram. Int. 39 (2013) 5651-5658.

[40] Z. Wang, D. Tao, G. Guo, S. Jin, F. Wei, W. Qian, S. Hong, J. Guo, Mater. Lett. 60 (2006) 3104-3108.

[41] A.R. Hajipour, Y. Ghayeb, N. Sheikhan, J. Iran. Chem. Soc. 7 (2010) 447-454.

[42] A.R. Hajipour, G. Azizi, Green Chem. 15 (2013) 1030-1034.

[43] A.R. Hajipour, A. Zarei, A.E. Ruoho, Tetrahedron Lett. 48 (2007) 2881-2884.

[44]A.R. Hajipour, A. Zarei, L. Khazdooz, B.B.F. Mirjalili, N. Sheikhan, S. Zahmatkesh, A.E. Ruoho, Synth. (2005) 3644-3648.

[45] A.R. Hajipour, A. Zarei, L. Khazdooz, S.A. Pourmousavi, B.B.F. Mirjalili, A.E. Ruoho, Phosphorus, Sulfur Silicon Relat. Elem. 180 (2005) 2029-2034.

[46] A. Zarei, A.R. Hajipour, L. Khazdooz, Tetrahedron Lett. 49 (2008) 6715-6719.

[47] A.R. Hajipour, L. Khazdooz, A.E. Ruoho, Catal. Commun, 9 (2008) 89-96.

[48] A.R. Hajipour, Z. Nasresfahani, Synth. Commun. 42 (2012) 1995-2006.

[49] A.R. Hajipour, Y. Ghayeb, N. Sheikhan, A.E. Ruoho, Tetrahedron Lett. 50 (2009) 5649-5651.

[50] A.R. Hajipour, M. Seddighi, Synth. Commun. 42 (2012) 227-235.

[51] P.B. Venuto, Microporous Mater. 2 (1994) 297-411.

[52] U. Sridevi, B.K. Bhaskar Rao, N.C. Pradhan, Chem. Eng. J. 83 (2001) 185-189.

[53] K. Becker, H. Karge, W.-D. Streubel, J. Catal. 28 (1973) 403-413.

[54] S.J. Gregg, K.S.W. Sing, Adsorption, Surface Area and Porosity, second ed., AcademicPress, New York, 1982.

[55] K. Segawa, S. Nakata, S. Asaoka, Mater. Chem. Phys. 17 (1987) 181-200.

[56] A. Tarafdar, A.B. Panda, N.C. Pradhan, P. Pramanik, Microporous Mesoporous Mater. 95 (2006) 360-365.

[57] M. Sawa, M. Niwa, Y. Murakami, Zeolites. 10 (1990) 532-538.

[58] H. Sato, Catal. Rev. 39 (1997) 395-424.

[59] K.i. Segawa, Y. Kurusu, Y. Nakajima, M. Kinoshita, J. Catal. 94 (1985) 491-500.

[60] S. Tahara, Y. Takakura, Y. Sugahara, Chem. Lett. 41 (2012) 555-557.

[61] X. Yang, X. Chen, L. Yang, W. Yang, Bioelectrochemistry 74 (2008) 90-95.

[62] K.S.N. Reddy, B.S. Rao, V.P. Shiralkar, Appl. Catal. A. 95 (1993) 53-63.

[63] R. Luque, V. Budarin, J.H. Clark, P. Shuttleworth, R.J. White, Catal. Commun. 12 (2011) 1471-1476.

[64] I. Graça, A. Fernandes, J.M. Lopes, M.F. Ribeiro, S. Laforge, P. Magnoux, F. Ramôa Ribeiro, Appl. Catal. A. 385 (2010) 178-189.

[65] P. Elavarasan, K. Kondamudi, S. Upadhyayula, Chem. Eng. J. 166 (2011) 340-347.

[66] Q. Zhao, Q. Wang, D. Wu, X. Fu, T. Jiang, H. Yin, J. Ind. Eng. Chem. 18 (2012) 1326-1331.

Highlights

- The catalyst has strong acid sites, high surface area and stability.
- 92% conversion of phenol with 88% selectivity toward 4-cyclohexylphenol were achived.
- The results showed that cyclohexanol is a better alkylating agent than cyclohexene.
- The catalyst was regenerated easily and reused five times without loss of activity.

Graphical Abstract

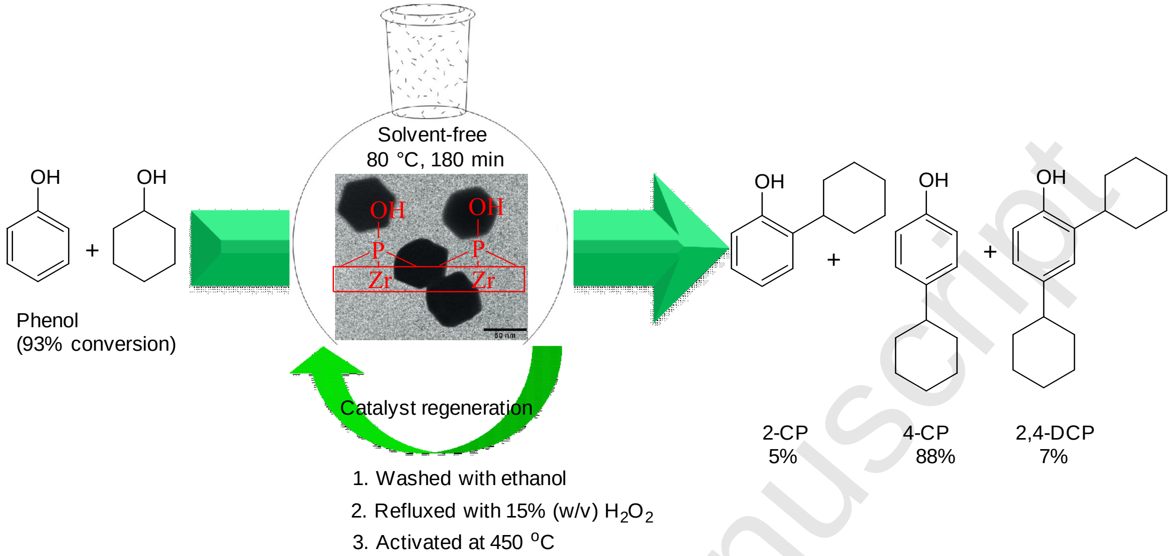

Schemes

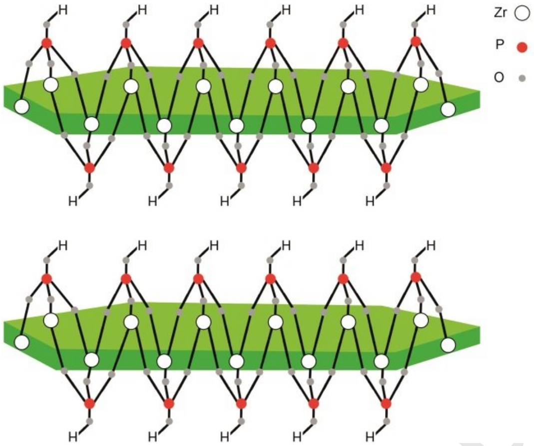

Scheme 1. Schematic structure of hexagonal α-zirconium phosphate.

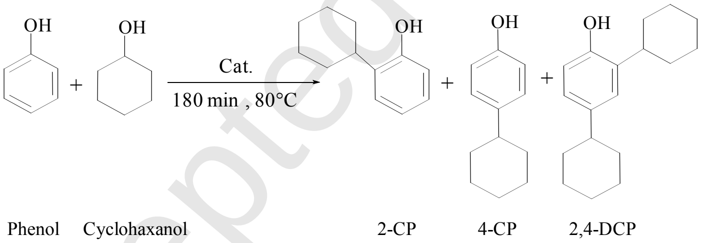

Scheme 2. The products of phenol alkylation with cyclohexanol under optimized reaction conditions.

Figures

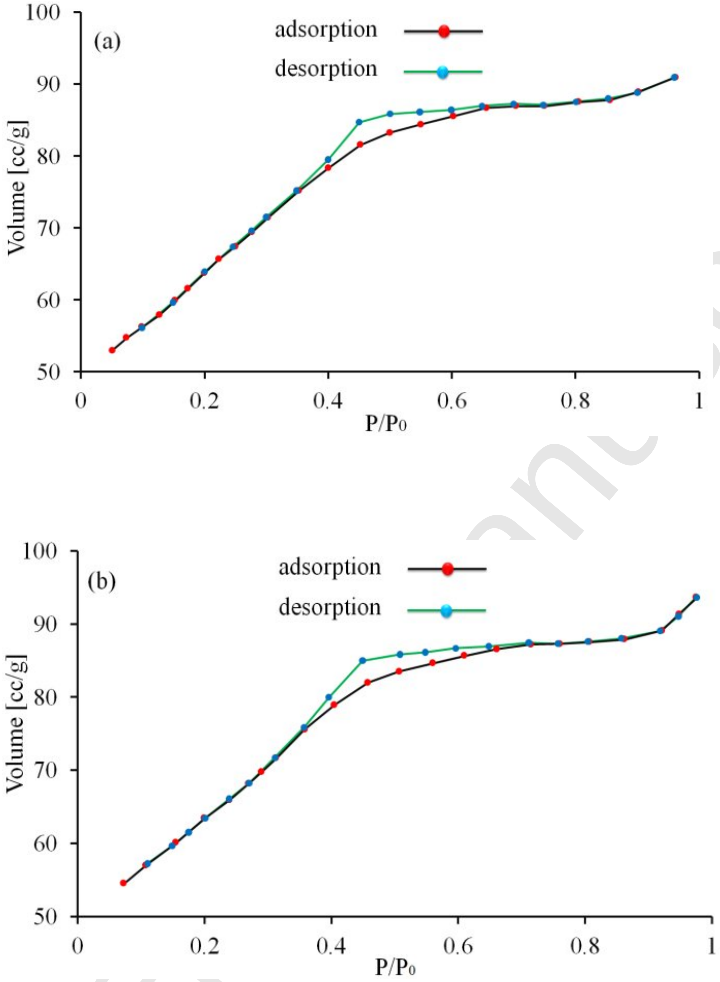

Fig. 1. Nitrogen adsorption–desorption isotherms for ZPA (a) and ZPP (b).

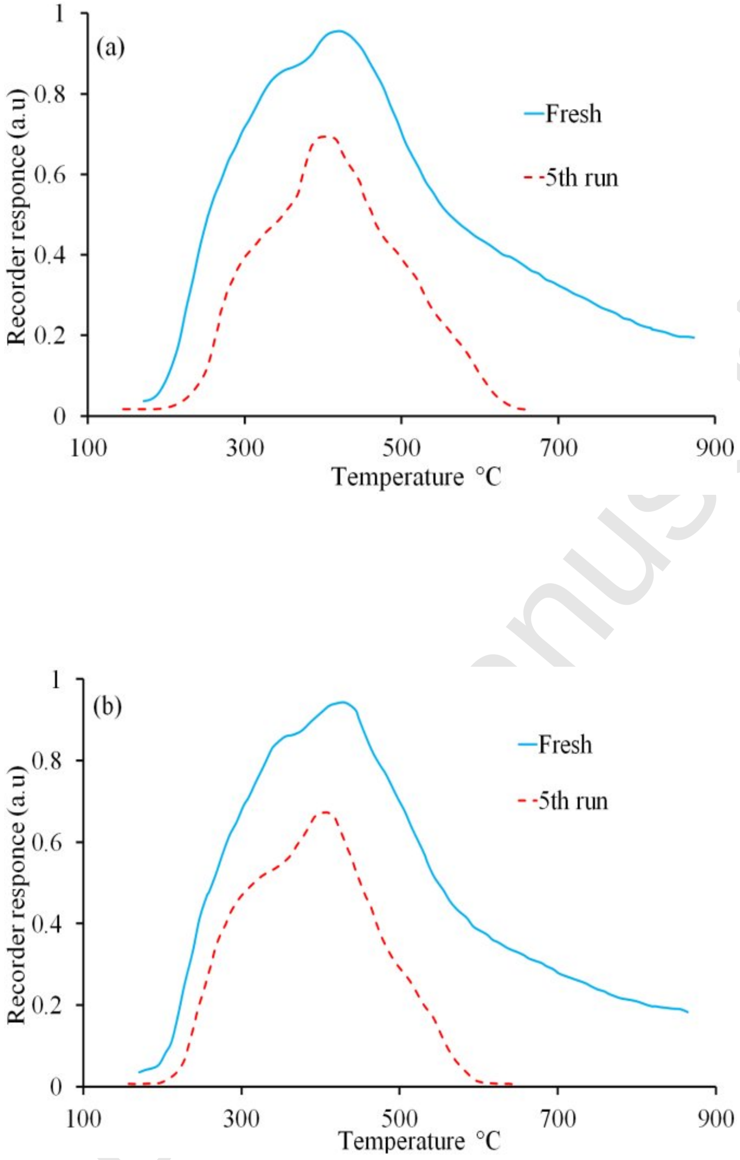

Fig. 2. NH_3 TPD profile of ZPA (a) and ZPP (b), fresh (blue line) and after the 5th run (red dashes).

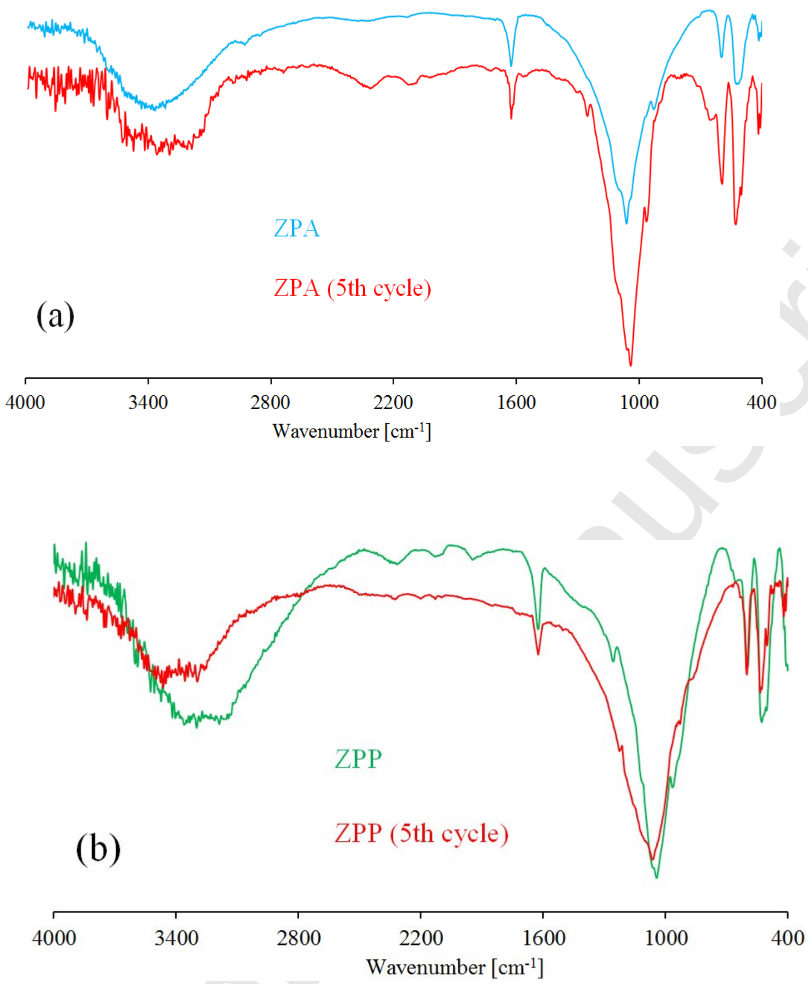

Fig. 3. FT-IR spectra of ZPA (a) and ZPP (b) before and after use.

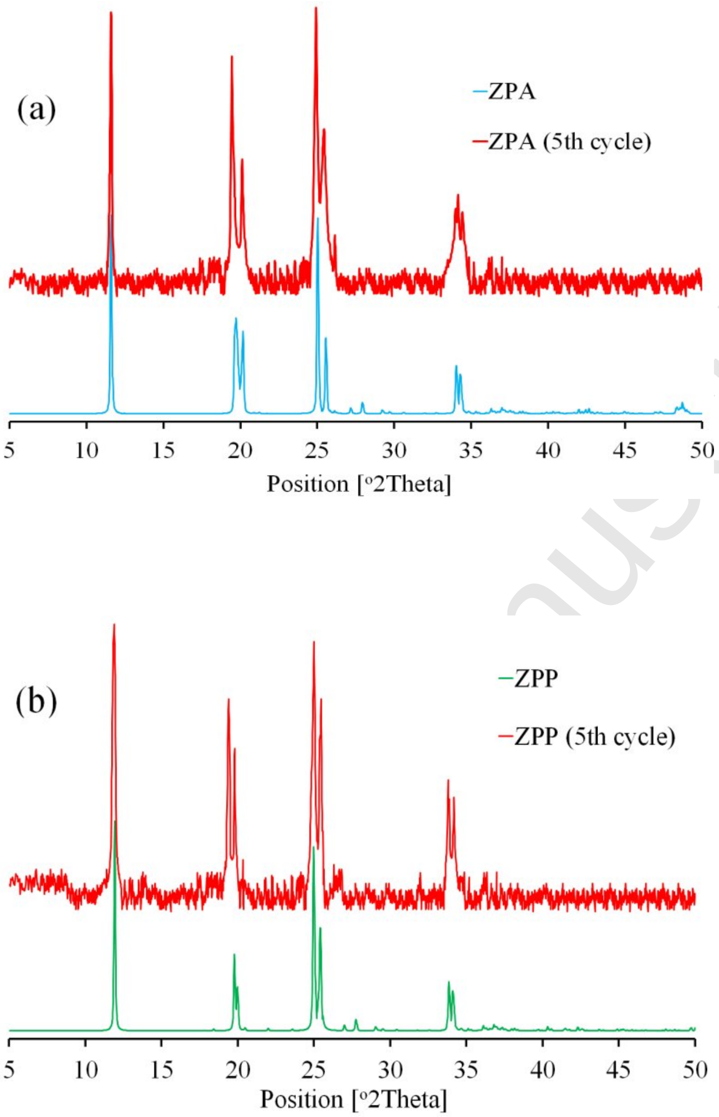

Fig. 4. XRD patterns of powder ZPA (a) and ZPP (b) before and after use.

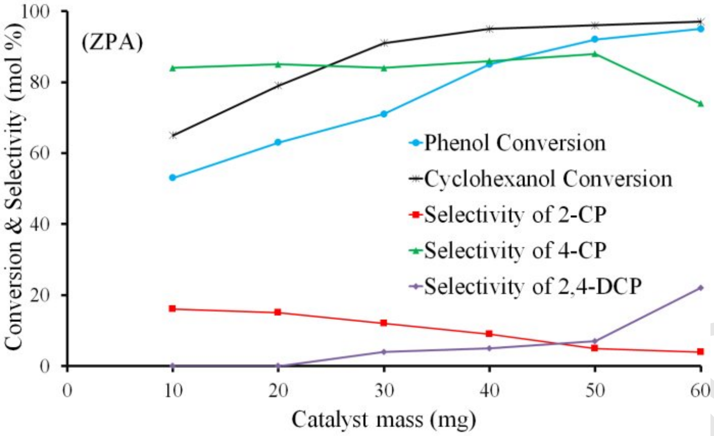

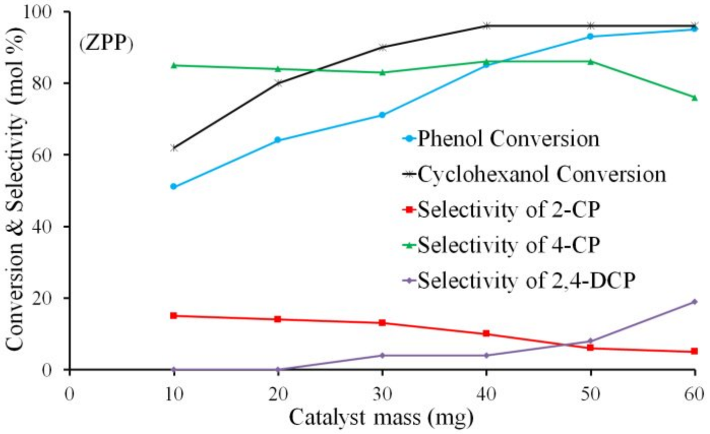

Fig. 5. Variation of reactants conversion and selectivity to main reaction products with ZPA and ZPP mass amount. The reaction conditions: phenol/cyclohexanol = 1:1, 180 min and 80 °C.

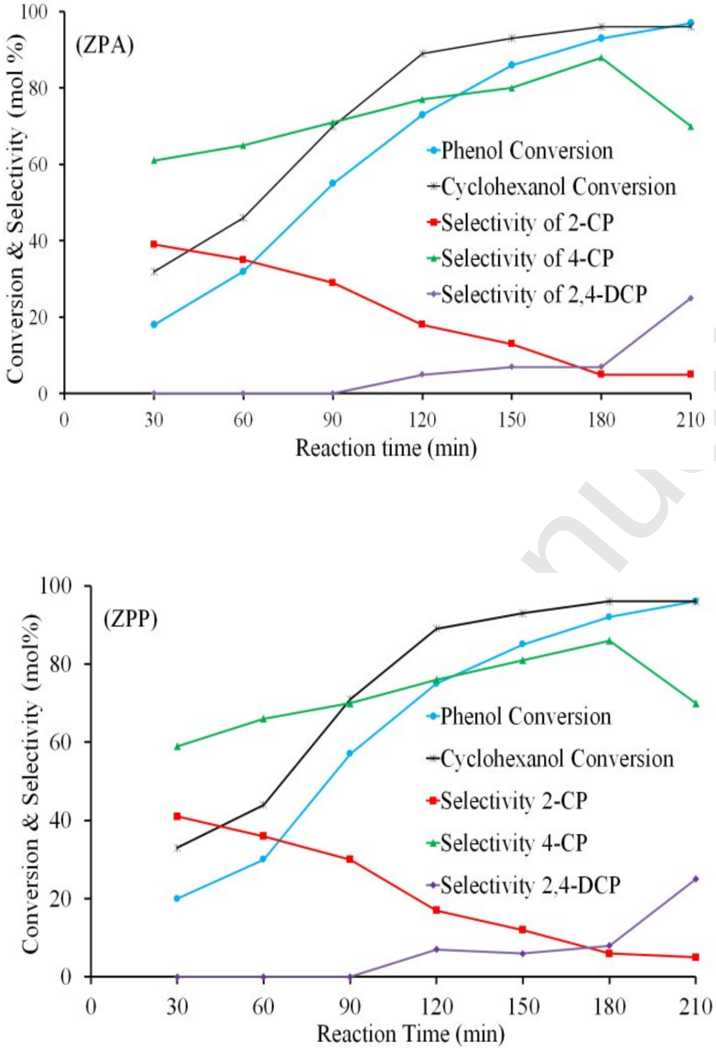

Fig. 6. Variation of reactants conversion and selectivity to main reaction products with time. The reaction conditions: phenol/cyclohexanol/catalyst = 1:1:0.017 and 80 °C.

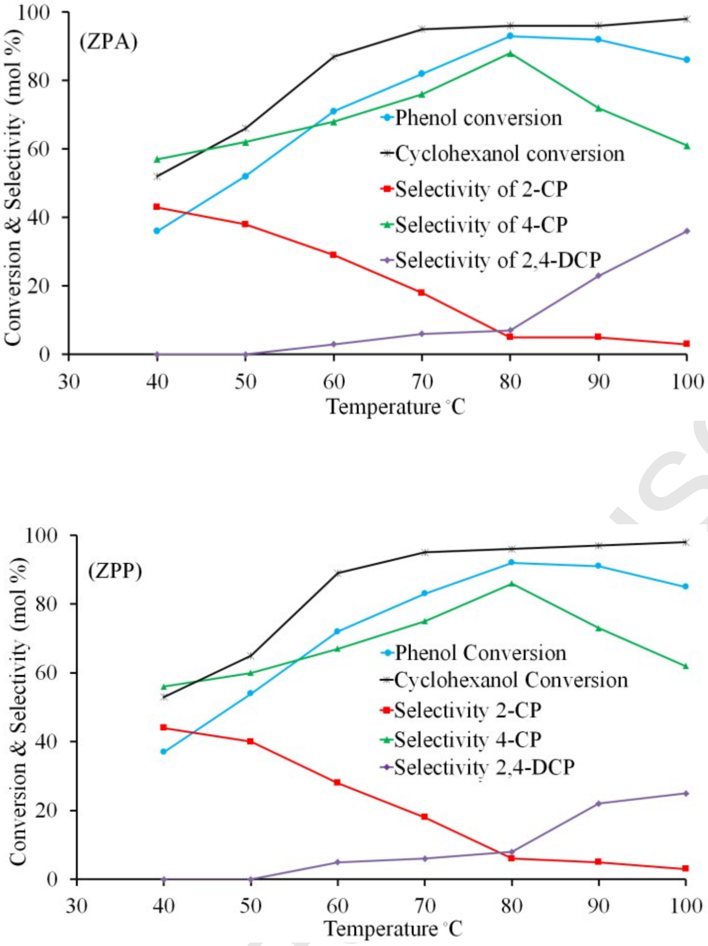

Fig. 7. Variation of phenol conversion and selectivity to main reaction products with reaction temperature. The reaction conditions: phenol/cyclohexanol/catalyst = 1:1:0.017 and 180 min.

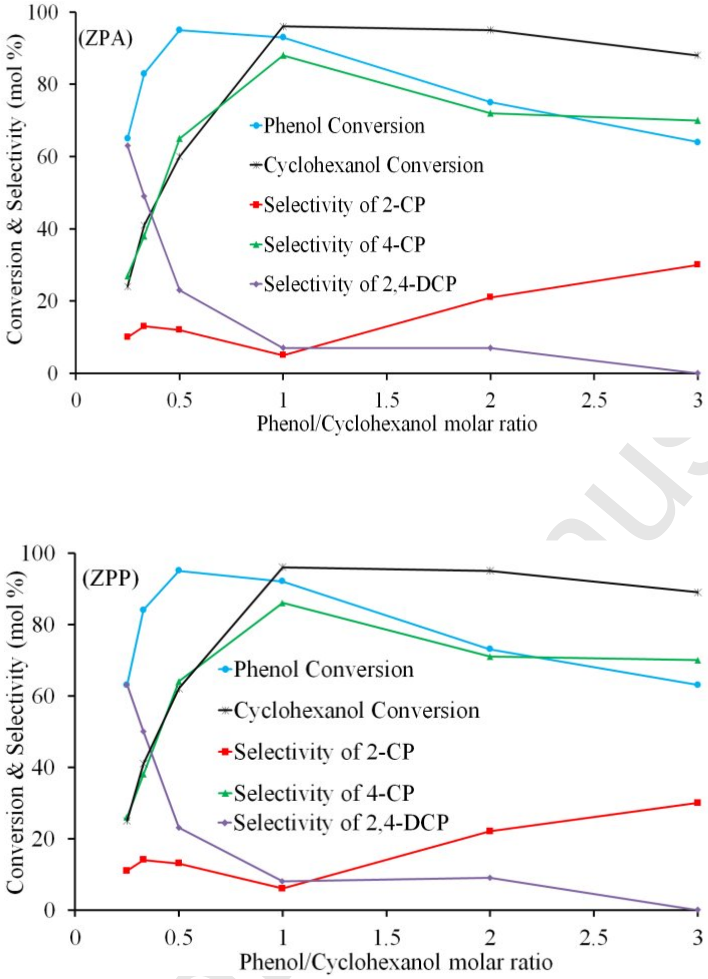

Fig. 8. Variation of reactants conversion and selectivity to main reaction products with reactants mole ratio. The reaction conditions: 180 min, 80 °C and 50 mg of catalyst.

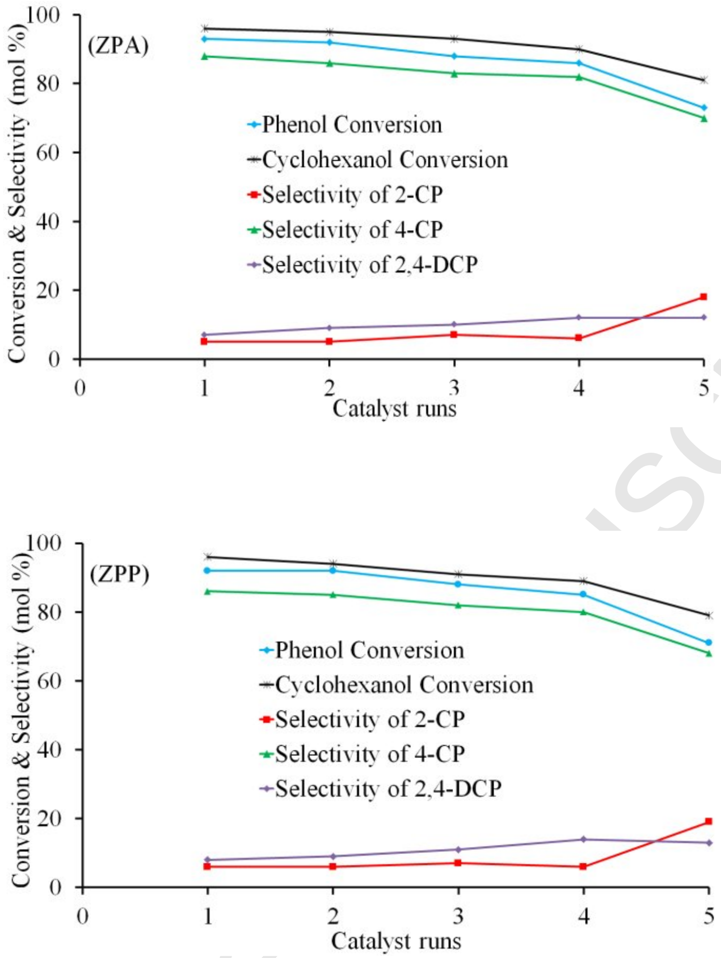

Fig. 9. Variation of reactants conversion and selectivity to main reaction products with reusability of ZPA and ZPP. The reaction conditions: phenol/cyclohexanol/catalyst = 1:1:0.017, 180 min and 80 °C.

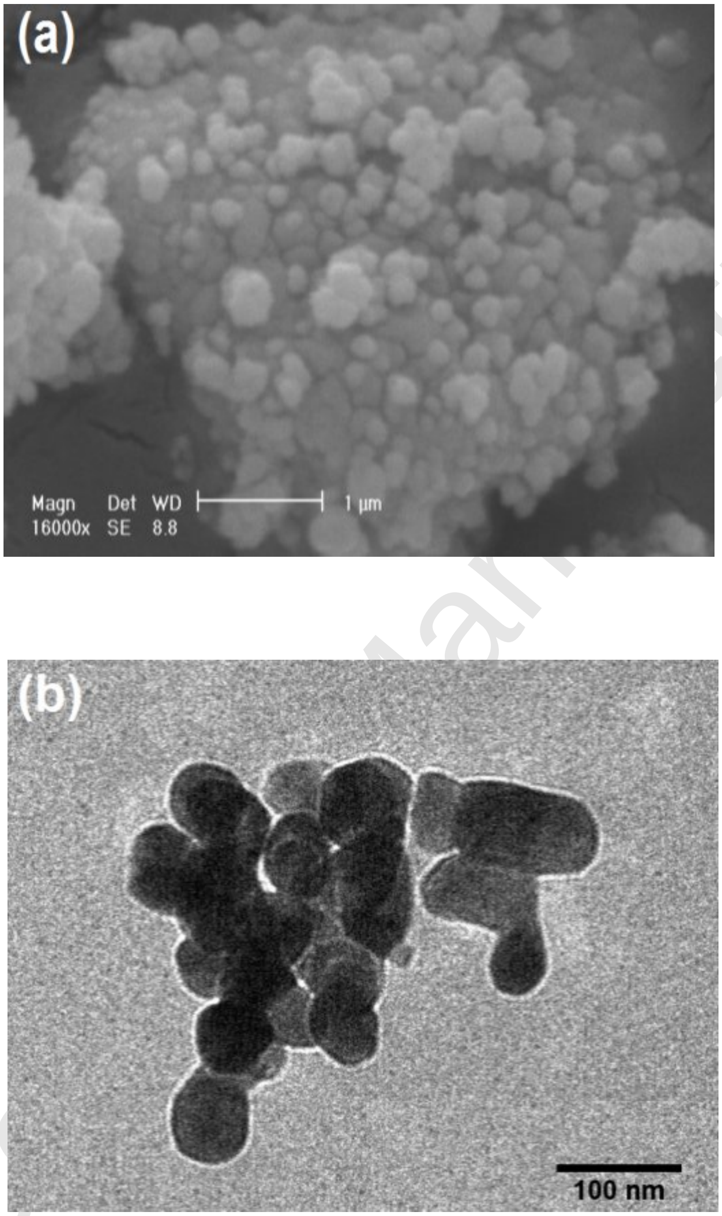

Fig. 10. SEM (a) and TEM (b) images of ZPA after the 5th run.